(36) Cohen, S. G.; Parola, A.; Parsons, J. H., Jr. *Chem. Rev.* **1973**, *73*, 141.
(37) Encina, M. V.; Sato, H.; Lissi, E. A. *J. Photochem.* **1974**, *3*, 467.
(38) Dalton, J. C.; Snyder, J. J. *J. Am. Chem. Soc.* **1975**, *97*, 5192.
(39) Yip, R. W.; Loufty, R. O.; Chow, J. L.; Magdzinski, L. K. *Can. J. Chem.* **1972**, *50*, 3426.
(40) Loufty, R. O.; Loufty, R. O. *Can. J. Chem.* **1972**, *50*, 4052.
(41) Abouin, E. B.; Encina, M. V.; Lissi, E. A.; Scaiano, J. C. *J. Chem. Soc., Faraday Trans. 1* **1975**, *71*, 1221.
(42) It has been reported that in the system benzophenone–amines, low photoreduction quantum yields are due to back reaction of ketyl and aminyl radicals: Inbar, S.; Linschitz, H.; Cohen, S. G. *J. Am. Chem. Soc.* **1980**, *102*, 1419.
(43) Rehm, D.; Weller, A. *Isr. J. Chem.* **1970**, *8*, 259.
(44) Ballardini, R.; Varani, G.; Indelli, M. T.; Scandola, F.; Balzani, V. *J. Am. Chem. Soc.* **1978**, *100*, 7219.
(45) Balzani, V.; Bolletta, F.; Scandola, F. *J. Am. Chem. Soc.* **1980**, *102*, 2152.
(46) Reference 26, p 290.
(47) Rozeboom, M. D.; Houk, K. N. *J. Am. Chem. Soc.* **1982**, *104*, 1189.
(48) Aue, D. H.; Webb, H. M.; Bowers, M. T. *J. Am. Chem. Soc.* **1976**, *98*, 311.
(49) Scaiano, J. C. *Chem. Phys. Lett.* **1981**, *79*, 441.
(50) Geuskens, G.; Baeyens-Volant, D.; Delaunois, G.; Lu Vinh, Q.; Piret, W.; David, C. *Eur. Polym. J.* **1978**, *14*, 291; **1978**, *14*, 299.
(51) Li, S. K. L.; Guillet, J. E. *Macromolecules* **1984**, *17*, 41.
(52) Ng, H.; Guillet, J. E. *Macromolecules* **1978**, *11*, 437.
(53) Scaiano, J. C.; Wubbels, G. G. *J. Am. Chem. Soc.* **1981**, *103*, 640.
(54) Stewart, L. C.; Carlsson, D. J.; Wiles, D. M.; Scaiano, J. C. *J. Am. Chem. Soc.* **1983**, *105*, 3605.
(55) Wismontski-Knittel, T.; Kilp, T. *J. Polym. Sci., Polym. Chem. Ed.* **1983**, *21*, 3209.
(56) Engel, P. S.; Woods, T. L.; Page, M. A. *J. Phys. Chem.* **1983**, *87*, 10.

Characterization of Epoxy Cure by UV–Visible and Fluorescence Spectroscopy: Azochromophoric Labeling Approach

Chong Sook Paik Sung,* Eumi Pyun, and Han-Li Sun

Department of Chemistry, Institute of Materials Science, University of Connecticut, Storrs, Connecticut 06268. *Received February 18, 1986*

ABSTRACT: Cure composition, reactivity ratio, activation energy, and weight-average molecular weight in two epoxy networks are investigated by an azochromophore labeling technique. The chromophore, *p,p'*-diaminoazobenzene (DAA), is used to mimic the reactivity of the curing agent, diaminodiphenyl sulfone (DDS). Reaction of DAA with epoxide produces red shifts, which have been deconvoluted on the basis of band assignments of model compounds. Thus, we obtain compositional analyses of cure products. Fluorescence due to the DAA label increases sharply due to the increasing fluorescence quantum yield of cure products containing tertiary amine rather than to viscosity changes. Fluorescence intensity has been used to estimate composition, based on kinetic differential equations, and these results have been compared with those obtained by UV–vis spectral deconvolution. Primary and secondary amines react at similar rates. The activation energy was estimated to be 16 kcal/mol on the basis of initial rate constants of the amine–epoxy reaction. Our experimental data were compared with the theoretically predicted weight-average molecular weight and soluble fractions. Finally, we compared UV–vis and IR techniques for the extent of cure in two epoxy systems. IR and thermal analyses suggest that DAA reacts a little faster than DDS. This difference in rates can be corrected by using a calibration curve.

Introduction

Recently, we reported a new method to obtain quantitative compositional information in the curing of epoxy with aromatic diamines by azochromophore labeling.[1] In this technique, we use a small amount of *p,p'*-diaminoazobenzene (DAA), which has reactivity similar to that of the curing agent diaminodiphenyl sulfone (DDS).[2] As the epoxy is cured, λ_{max} of the $\pi \rightarrow \pi^*$ transition corresponding to the azo bond of DAA is red-shifted in a way that provides spectral discrimination for the cure products (cross-linkers, branch points, linear chains, chain ends, and unreacted diamines).

The accuracy of our compositional analyses depends on the proper assignments of λ_{max} positions and the determination of the extinction coefficients for the various cure products. For this objective, we will first describe our attempt to make and separate model compounds by reacting DAA with a monoepoxy compound (glycidyl phenyl ether). We will use λ_{max} positions and extinction coefficients obtained from these model compounds in the deconvolution of the UV–vis spectra.

We have studied two epoxy networks in this work: DGEBA–DDS epoxy has a maximum T_g of 215 °C, which leads to a complete cure subject to degradation.[3] Furthermore, when this network is cured below 215 °C, vitrification occurs some time after gelation (e.g., 150 min at a cure temperature of 160 °C) according to its T–T–T diagram.[3] Since there is little progress in the cure reaction after vitrification, the extent of cure is also limited. Therefore, we chose another epoxy, DGEB–DDS epoxy (diglycidyl ether of butanediol–DDS), which has a maximum T_g of about 80 °C.[4] This epoxy when cured above 80 °C will gel but will not vitrify, thus pushing the cure extent almost to completion.

From these two epoxy networks cured at three isothermal temperatures, we have obtained a quantitative composition of each cure product covering a wide range of cure extents. With such experimental data, we first attempt to determine the reactivity ratio of the primary and secondary amines with the epoxy group. This ratio is predicted to have a strong effect on the cure process, including parameters such as gel time, molecular weight, and the elastically active network chains.[5-7] From the initial slopes of the rate constants of epoxy–primary amine reaction vs. the reciprocal temperature, we attempt to estimate the activation energy. Second, our data are compared under a certain assumption with the prediction of weight-average molecular weight as a function of cure by using Miller and Macosko's recursive theory for network.[7] Predicted soluble fractions are also compared with the composition of cure products.

We recently discovered that the total fluorescence intensity by the DAA label at 560 nm increases sharply as the cure proceeds.[9] This behavior is not due to the viscosity change, but rather to the increasing fluorescence by the cure products. The observed fluorescence intensities

0024-9297/86/2219-2922$01.50/0

Table I
Physical Characteristics of the Fractions Obtained by Reaction of DAA and GPE

fraction	color	mp, °C	mass spec	nitrogen (calcd[a]/obsd)	UV–vis,[b] μm
A	brown	<70	MW 365 obsd	15.46/13.79	420
B	reddish	185–186	MW 512 obsd	10.93/10.75	445
C	yellowish	177	MW 662 (small peak) obsd	not enough for analysis	458
D	orange	172	not available	6.39/6.49	460

[a] Calculated on the assumption that fractions A, B, and D correspond to model compound 1, 2 (or 3), and 5, respectively. [b] The main λ_{max} is indicated; there were shoulders present in some fractions. The extinction coefficient at the main peak was about 4×10^4 mol/cm, independent of the fractions.

per mole of the model compounds representing each cure product are in the following ratios when the compounds are excited at 456 nm: cross-linker (1400); branch point (1100); linear chain (18); chain end (9); and DAA (1). Assuming the above ratios and using the known concentration of each cure product by deconvolution of UV–vis spectra, we observed that overall fluorescence intensity can be modeled as the sum of contributions from each cure product. Thus, fluorescence can be used to monitor cure reactions in DAA-labeled epoxy. We also compared the extent of cure between DGEBA–DDS and DGEB–DDS epoxies by the fluorescence method. Furthermore, using the ratio of the amine functionalities estimated from UV–vis data, we have estimated the composition of cure products at a given fluorescence intensity value. The results are compared with those obtained by UV–vis spectral deconvolution.

Experimental Section

Synthesis of Model Compounds. *p,p'*-Diaminoazobenzene (DAA) from Eastman Kodak Chemical was purified by passing it through basic alumina columns. This method of purification left little residue in a TLC plate in comparison to the DAA recrystallized from toluene and acetone. Purified DAA had a melting point in the range 238–241 °C. 1,2-Epoxy-3-phenoxypropane (glycidyl phenyl ether, GPE) from Aldrich was used without further purification.

Model compounds were made by reacting DAA and GPE at 145 °C under N_2 with a varying excess of GPE. Scheme I shows the chemical structures of the major model compounds expected from this reaction. In order to obtain intermediate cure products, DAA and GPE were reacted in 1:4 molar ratio for 10 or 30 min at 145 °C. After the reaction products were developed with a mixture of benzene:acetone:diethylamine (16:3:1) five times, three well-separated spots in a TLC plate were seen. The top spot corresponds to DAA; the two lower spots (fractions A and B) were purified, and their properties are summarized in Table I. In order to obtain products of the later stages of the reaction, DAA was reacted with a large excess of GPE (6-, 8-, or 30-fold excess) for periods up to 4 h at 150 °C under nitrogen. The major reaction products (fractions C and D) appeared between fractions A and B after developing four times with a 13:1:1 mixture of benzene:acetone:diethylamine. The reaction mixture was initially fractionated by flash chromatography using silica gel at a pressure of 25 lb/in^2 with the same solvent mixture described above. Of the total fractions collected from flash chromatography, mother liquids of fractions 11–19 were combined after a 1:1 mixture of petroleum ether and ethanol was added to precipitate an orange powder. Preparatory TLC was used to separate fractions C and D from this mother liquid by the same solvent mixture after developing eight times. Their physical characteristics are summarized in Table I.

HPLC Analyses. Fractions A–D obtained from model reactions were further analyzed by reversed-phase HPLC using a Waters Associates analytical system interfaced with a Spectra Physics data system. Reversed-phase (Bondapak C_{18}) columns were employed, using solvent programmer gradient and varying amounts of acetonitrile in water. An ultraviolet detector set at 280 nm was used.

DAA Labeling Studies in Epoxy. DGEBA was recrystallized from saturated MEK solution by seeding it with purified DGEBA crystal and leaving it in the freezer (−15 °C) for 1–2 weeks. DAA was purchased from Eastman Kodak and recrystallized from toluene and acetone. DDS and DGEB, which were purchased from Aldrich, were used without purification. In typical cure monitoring studies, a small amount of DAA (5–7 mg or about 0.1% by weight for UV–vis studies and 0.01% by weight in most fluorescence studies) was mixed with a stoichiometric mixture of DGEBA (5.0 g) or DGEB (2.98 g). DDS (1.825 g) was then added, and the mixture was heated with a magnetic stirrer at 120 °C for 5 min. Two circular quartz plates were clamped together with two thin Mylar films (1.5 mil) on the edges, leaving a center space for the sample. The clamped quartz plate with Mylar spacers was dipped into epoxy heated to 100 °C, and the sample went into the center space by capillary action. UV–vis spectra and fluorescence spectra were measured after the sample was cured in an oven for a specific time and cooled to room temperature. Fluorescence was measured by using a 1-nm-wide excitation slit and a 10-nm-wide emission slit on a Perkin-Elmer MPF-66 spectrometer with a Model 7500 data station. UV–vis spectra were obtained with a Perkin-Elmer diode array (Model 3840) system with a Model 7500 data station. As will be discussed in the next section, the total area under the UV–vis peak for the label remains constant as long as the thickness does not change, due to the same extinction coefficients observed for cure products of DAA. Therefore, we used the total UV–vis peak area to calibrate for thickness fluctuations during cure to obtain the relative fluorescence intensity. UV–vis spectra were deconvoluted with a computer program[8] assuming a Gaussian distribution curve for each cure species. The λ_{max}'s of the various cure products were assigned 410, 420, 445, 460, and 470 nm, respectively.

Scheme I
Chemical Structure of Model Compounds

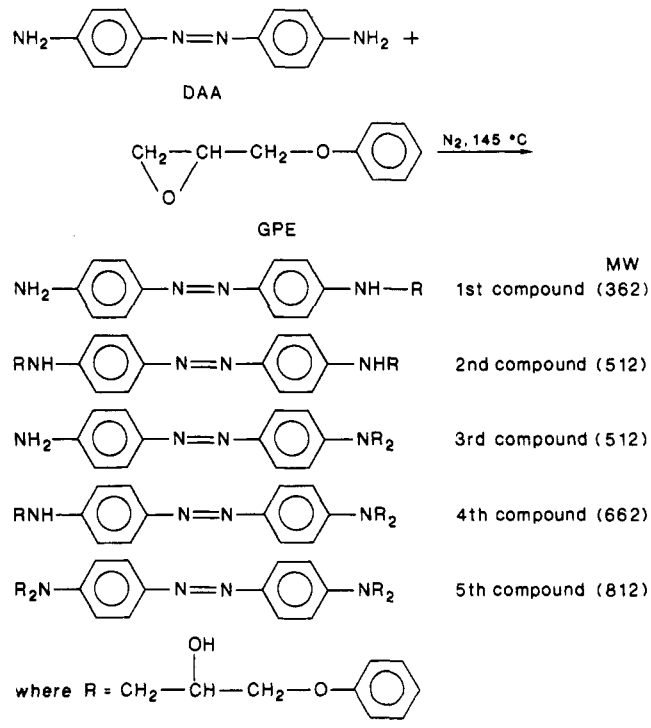

Results and Discussion

1. Model Compounds. Table I shows the physical characteristics of fractions A–D. There is a distinct color

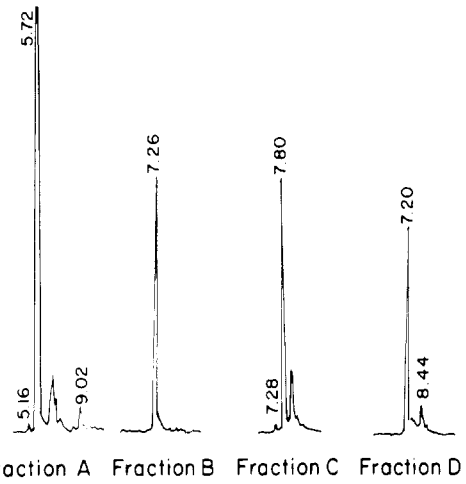

Figure 1. Reversed-phase liquid chromatography traces for fractions A–D from reactions of phenyl glycidyl ether and diaminoazobenzene.

change as the fractions change from A to D. Fraction A is brownish as is DAA itself, while fraction B is reddish. Fractions C and D are yellow and orange, respectively. Results of nitrogen analyses are close to the calculated results, assuming that fraction A, B, or D corresponds to model compound 1, 2, or 5, respectively, as shown in Scheme I. Mass spectroscopic results were inconclusive, and the UV–vis spectrum shows shoulders in addition to the main absorption peak. In order to ascertain if fractions A–D are pure, we carried out reverse-phase high-pressure liquid chromatography using mixtures of acetonitrile and water as the mobile phase. Figure 1 shows their HPLC profiles. All the samples including DAA and GPE except fractions C and D were obtained under the same conditions (e.g., starting gradient of acetonitrile/water = 50/50). For C and D, a different gradient (70/30) was used. DAA appears at 3.52 (76%), while GPE appears at 3.80. Fraction A shows a main peak at 5.72 (91%) and several small impurity peaks (<2% each). Fraction B shows its main peak at 7.26 (95%). The fact that the fractions A and B occur at higher evolution volume than that for DAA is consistent with the trend observed by TLC. Fraction C shows four peaks between 7 and 9, with two major peaks at 7.80 (68%) and 8.48 (16%). Fraction D shows a main peak at 7.20 (81%) and a small peak at 8.44 (7%). While fractions A and B are relatively pure, fractions C and D are certainly mixtures. We attempted to spread closely overlapping peaks for fractons C and D by using a different starting gradient (80/20 ratio of acetonitrile to water). After the major peak was separated, the UV–vis scan was taken in the HPLC instrument by switching the UV–vis detector to the scanning mode. The maximum absorption for the major peak for fractions C and D is about 460 and 470 nm, respectively. For fractions A and B, the absorption maxima were 420 and 445 nm, respectively. Since fraction B is quite pure, it could be either model compound 2 or 3. At this time, we cannot distinguish between them. Therefore we used these λ_{max} positions as summarized in Table II in the deconvolution of the peaks obtained in epoxy system. The extinction coefficient of about 4×10^5 mol/cm was measured regardless of the fractions. Thus, we assumed equal extinction coefficient in the deconvolution of the curves.

2. Cure Composition from UV–vis Studies. Figure 2 compares UV–vis spectra obtained as a function of cure time in DGEB–DDS and DGEBA–DDS at 160 °C. In both sets of spectra, significant red shifts of DAA derivatives are observed with increasing cure time. The conversion

Table II
Positions of λ_{max} for Model Compounds of DAA and GPE

model compd[a]	λ_{max}, nm	$\Delta\lambda$
DAA (pp)	410	0
1 (ps)	420	10
2 (ss), 3 (pt)	445	35
4 (st)	460	50
5 (tt)	470	60

[a] Refer to Scheme I for chemical structure. Designation in parentheses: p means primary amine, s means secondary amine, and t means tertiary amine.

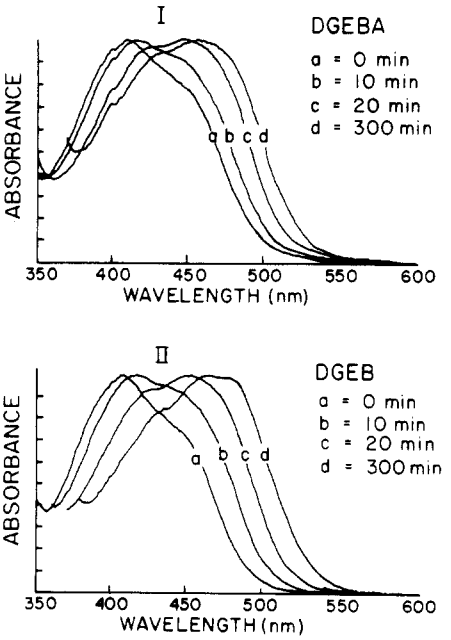

Figure 2. UV–vis spectra of *p,p'*-diaminoazobenzene (DAA) in a stoichiometric mixture of DGEBA–DDS (I) and DGEB–DDS (II) as a function of cure time at 160 °C.

of DDS to tertiary amine also red-shifts the absorption of epoxy matrix, resulting in the minimum point of the spectra from 360 to 380 nm. In DGEBA–DDS epoxy, the matrix gels after about 50 min of cure and vitrifies after 150 min of cure according to the T–T–T diagram at this cure temperature.[3] After vitrification, the cure reaction is supposedly quenched. As a consequence, UV–vis spectra in the DGEBA–DDS matrix do not show much change after vitrification (see Figure 2Id corresponding to 300-min cure time). In contrast, no vitrification occurs at 160 °C in DGEB–DDS epoxy since its maximum T_g is only about 80 °C. The cure reaction has been pushed further as indicated by additional red shifts shown in Figure 2IId for the DGEB–DDS epoxy. Epoxy ring disappearance monitored by IR provides support for this trend in DGEB–DDS, which will be discussed in the last section of this paper.

In order to ensure that these spectral shifts are due to cure reactions and not to changes in the matrix (e.g., polarity change as a function of cure), we ran UV–vis spectra of the model compound representing cross-linkers in DGEBA–DDS epoxy as a function of cure at 160 °C. Any spectral shift in this case would be due to the matrix change since the cross-linkers cannot react any further. Only a negligible (<5 nm) spectral shift was observed. Therefore, we interpret the spectral shifts obtained in DAA-labeled epoxy as arising from cure reactions only.

Table III summarizes the results on the composition of cure products by deconvolution of UV–vis spectra with a computer program assuming λ_{max} positions of the model cure products according to Table II and a Gaussian dis-

Table III
Composition of Cure Products in DGEB-DDS and DGEBA-DDS Epoxies as a Function of Cure Time at 160 °C

cure time, min	cure products, %					extent of amine reaction (ξ_a)
	A_{pp}	A_{ps}	A_{ss}	A_{st}	A_{tt}	
			DGEB-DDS			
0	78	20	2	0	0	0.059
5	44	34	14	6	2	0.219
10	33	33	16	11	7	0.318
20	13	20	32	22	14	0.510
30	6	12	20	31	31	0.676
45	2	8	18	33	40	0.750
70	2	4	17	36	41	0.775
100	1	5	13	30	52	0.815
150	1	5	11	21	62	0.848
300	1	3	10	37	47	0.814
800	1	3	13	34	49	0.813
			DGEBA-DDS			
0	75	25	0	0	0	0.063
5	61	20	9	6	5	0.183
10	35	41	9	9	5	0.270
15	25	28	36	5	5	0.343
30	10	17	17	23	34	0.636
45	8	10	23	25	33	0.653
60	9	15	19	25	33	0.646
100	10	15	26	25	23	0.667
150	10	15	15	29	27	0.675
300	8	14	23	29	27	0.638
1140	7	20	12	20	42	0.680

tribution curve for each species. The error in resolving closely overlapping peaks as in our spectra can be significant, especially when the cure is intermediate (e.g., Figure 2b,c). We tried to fit the curve until the overall error calculated by the program was below 2%. Still, we estimate that the error in the composition of each cure product can be possibly as large as 10%, since the composition, given in Table III, corresponding to a certain cure time may not be a solution unique to the particular spectrum. The last column of Table III lists the extent of amine reaction (ξ_a) as defined by the equation

$$\xi_a = [A_{ps} + 2(A_{ss} + A_{pt}) + 3A_{st} + 4A_{tt}]/4 \qquad (1)$$

where A_{ps}, A_{ss}, A_{pt}, A_{st}, and A_{tt} correspond to the fractional amounts of cure products as defined by Scheme II. A_{pp} is the fraction of unreacted diamine. From Table III, we can obtain the following trends: (1) As predicted by the spectral shifts of Figure 2, the fraction of branch points and cross-linkers increases with cure time for both epoxy matrices. (2) Cure reaction for DGEBA-DDS epoxy seems somewhat slower than for DGEB-DDS, especially at long cure times. This is shown by the values of the cure products as well as in Figure 3, which compares the overall extent of amine reaction (ξ_a) vs. cure time for both epoxy systems when they are cured at 160 °C. Figure 3 also reveals an interesting phenomenon. In DGEBA-DDS, the maximum ξ_a is only about 70%, presumably due to quenching by vitrification. Even in DGEB-DDS where vitrification does not occur at the cure temperatures, ξ_a only reaches about 85% at this temperature.

Figure 4I, II shows the cure temperature dependence on the extent of amine cure for both epoxy systems. At an early stage of the cure, the effect of higher temperature is quite pronounced, leading to a greater cure extent. At later stages of cure, the temperature does not have much effect, especially for DGEBA epoxy, leading to similar plateau values in the overall extent of reaction. This phenomenon is partly due to the vitrification occurring in DGEBA epoxy in comparison to the absence of vitrification in DGEB epoxy. However, one would expect higher plateau values at higher cure temperatures (e.g., 180 °C) since the extent of reaction at vitrification is temperature dependent. We will discuss the reason for the observed similarity in the plateau values in the last section of this paper when we compare the extent of amine (DAA) reaction with that of the epoxy reaction. Similar s-shaped curves with a plateau at high extent of conversion are also reported by DSC isothermal cure studies for another DGEBA–amine system.[10] It is noted in Figure 4II that the maximum ξ_a obtained for DGEB-DDS is about 95% when it is cured at 180 °C.

Scheme II
Kinetic Scheme of Epoxy Cure Reactions

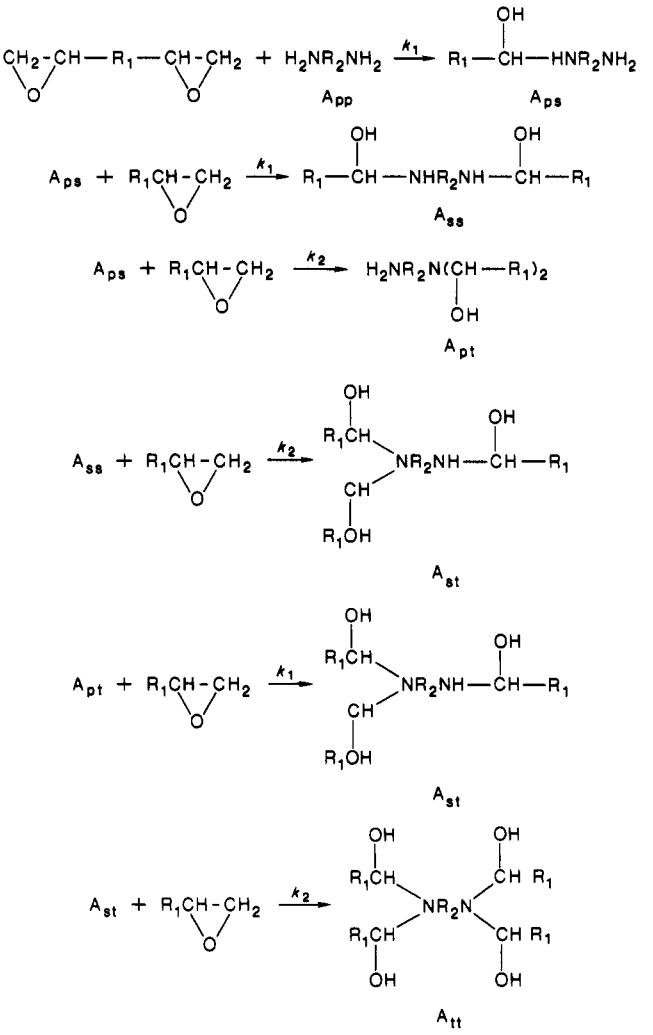

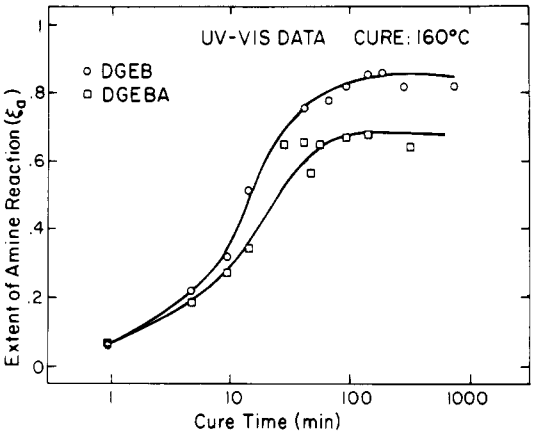

Figure 3. Extent of amine reaction (ξ_a) plotted as a function of cure time at 160 °C for DGEBA-DDS and DGEB-DDS.

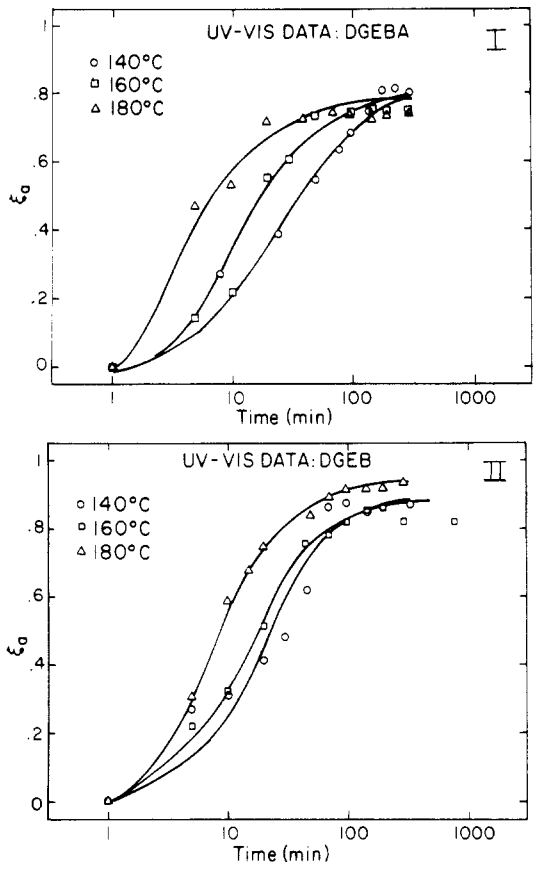

Figure 4. Temperature dependence of the extent of amine reaction, ξ_a, as a function of cure time: (I) DGEBA–DDS; (II) DBEB–DDS.

3. Kinetic Analyses of Epoxy Cure. Since epoxy homopolymerization may be neglected in the absence of catalysts,[11] the major cure reactions can be assumed to be the reactions between epoxide and amine groups as expressed in Scheme II. This kinetic scheme defines the rate constant k_1 due to the conversion of primary amine to secondary amine, while k_2 is due to the conversion of secondary amine to tertiary amine.

On the basis of Scheme II, one can write a series of kinetic differential equations as described by Dusek et al.[5]

$$-\mathrm{d[pp]}/dt = 4k_1[\mathrm{pp}][\mathrm{b}] \quad (2)$$

$$-\mathrm{d[ps]}/dt = 2k_1[\mathrm{ps}][\mathrm{b}] + k_2[\mathrm{ps}][\mathrm{b}] - 4k_1[\mathrm{pp}][\mathrm{b}] \quad (3)$$

$$-\mathrm{d[ss]}/dt = 2k_2[\mathrm{ss}][\mathrm{b}] - 2k_1[\mathrm{ps}][\mathrm{b}] \quad (4)$$

$$-\mathrm{d[pt]}/dt = 2k_1[\mathrm{pt}][\mathrm{b}] - k_2[\mathrm{ps}][\mathrm{b}] \quad (5)$$

$$-\mathrm{d[st]}/dt = k_2[\mathrm{st}][\mathrm{b}] - 2k_2[\mathrm{ss}][\mathrm{b}] - 2k_1[\mathrm{pt}][\mathrm{b}] \quad (6)$$

$$-\mathrm{d[tt]}/dt = -k_2[\mathrm{st}][\mathrm{b}] \quad (7)$$

where [b] is the concentration of unreacted epoxy groups.

By solving the above equations, we can obtain the fraction of each cure species as a function of the reactivity ratio of k_2/k_1 and the fraction of unreacted diamine (A_{pp})

$$A_{ps} = 2p(A_{pp}^{q} - A_{pp}) \quad (8)$$

$$A_{ss} = p^2(-2A_{pp}^{q} + A_{pp} + A_{pp}^{r/2}) \quad (9)$$

$$A_{pt} = -2pA_{pp}^{q} + rpA_{pp} + 2A_{pp}^{1/2} \quad (10)$$

$$A_{st} = p^2[(r+2)A_{pp}^{q} - rA_{pp} - (2-r)A_{pp}^{1/2} - 2A_{pp}^{r/2} + (2-r)A_{pp}^{r/4}] \quad (11)$$

$$A_{tt} = p^2[-rA_{pp}^{q} + (r^2/4)A_{pp} + (r/p)A_{pp}^{1/2} + A_{pp}^{r/2} - (2-r)A_{pp}^{r/4} + (r/2-1)^2] \quad (12)$$

where $r = k_2/k_1$, $p = 1/(1 - r/2)$, and $q = (1 + r/2)2$

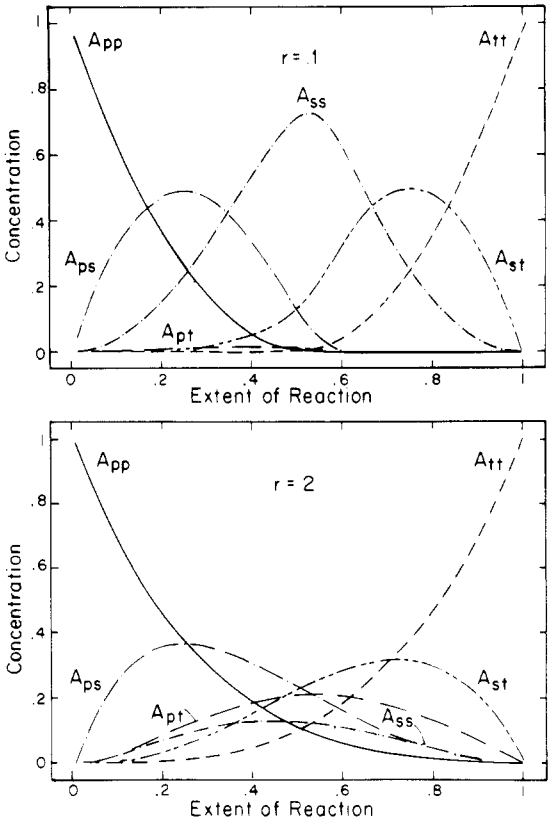

Figure 5. Theoretical prediction of the composition of cure species as a function of amine reaction (ξ_a) according to eq 8–12 for two different reactivity ratios (0.1 or 2).

The overall extent of amine reaction (ξ_a) as defined before can now be written in terms of A_{pp} and r only, as follows:

$$\xi_a = 1 - [1/(2-r)][(1-r)A_{pp}^{1/2} + A_{pp}^{r/4}] \quad (13)$$

Now we can plot a calculated fraction of each cure product and of the unreacted diamine as a function of ξ_a as shown in Figure 5. In the top panel of Figure 5, the reactivity ratio, r, is assumed to be 0.1, while the bottom panel represents the case of $r = 2$. In a comparison of these two figures, it becomes obvious that the smaller the r value, the greater the magnitude of A_{ps}, A_{ss}, and A_{st}. When $r = 2$, A_{pt} becomes noticeable, while it is negligible when r is less than one. Also at smaller values of r, A_{pp} decreases rapidly, while A_{tt} increases more slowly than at greater values of r.

Now we attempt to determine the r value that best fits with the experimental data. As demonstrated by the branching theory of Bidstrup and Macosko[6] and Dusek,[5,7] the r value has a strong effect on many structural parameters of the network. From the UV–vis spectra obtained at three cure temperatures (140, 160, and 180 °C), the fraction of each cure product was deconvoluted and plotted with the maximum error bars as a function of the extent of amine reaction in Figure 6I,II. As shown in Figure 6I, experimental data are only available up to about 75% reaction due to vitrification occurring in DGEBA–DDS epoxy. In contrast, experimental data are available up to 95% reaction in DGEB–DDS epoxy.

In the literature, many values of r have been reported.[12,13] While the majority of the reported r values are close to one, much smaller r values in the range 0.1–0.2 were also reported.[14,15] In fact, r of 0.1 was sometimes used by the theoreticians.[6] One of our primary objectives in this work was to clarify the confusion concerning the reported r values.

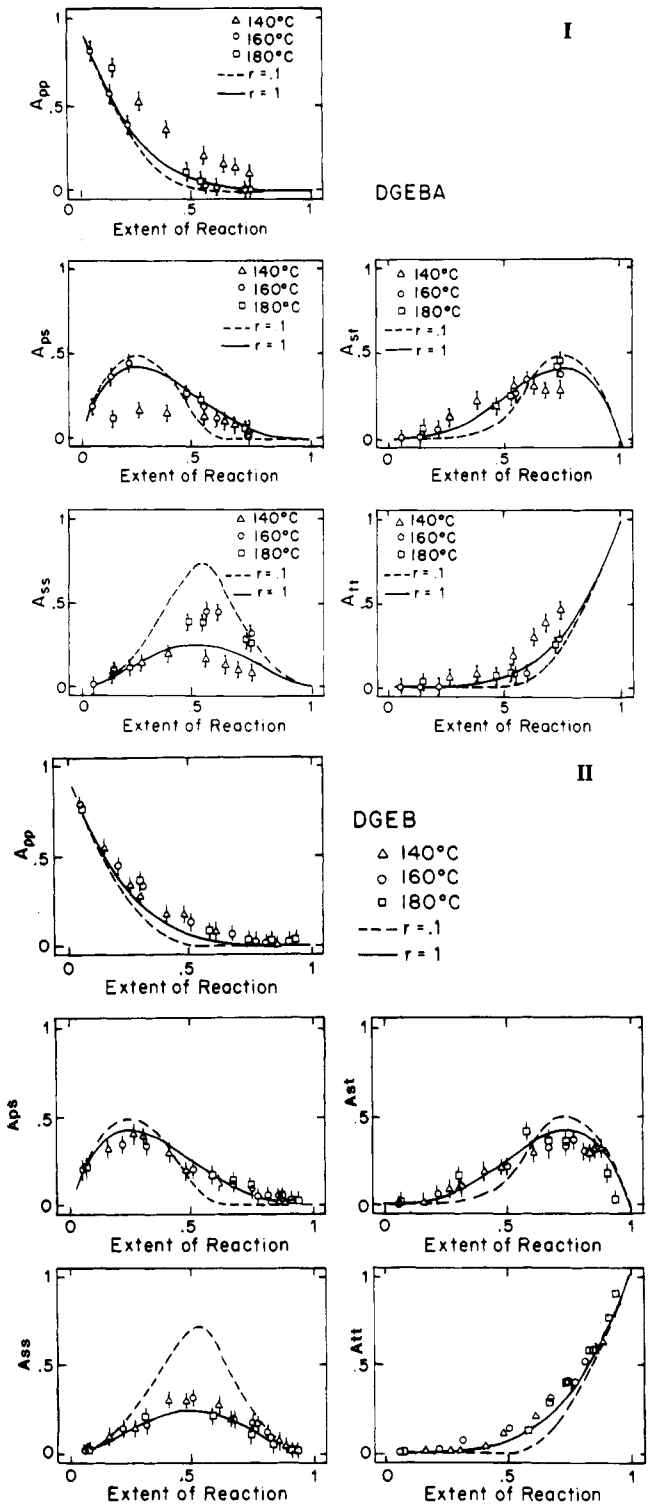

Figure 6. Experimental composition of cure species as a function of extent of amine reaction for DGEBA–DDS (I) and DGEB–DDS (II). Data from several cure temperatures have been combined. Two dotted lines show predictions for reactivity ratio of either 0.1 or 1.

In order to find the best-fit value of r, we show two theoretical curves according to the eq 8–12 corresponding to r of 0.1 (dotted line) or 1 (solid line). Comparison between experimental data with these two sets of curves, especially the A_{ss} profile, clearly eliminates the possibility of being close to 0.1. In fact, an r value of unity seems to fit the data quite well, especially for DGEB–DDS epoxy. Thus, reaction rates of primary amine–epoxy and secondary amine–epoxy are practically indistinguishable. This is also the conclusion reached by Prime[16] after a careful review of the literature and especially in view of the thermal analyses data.

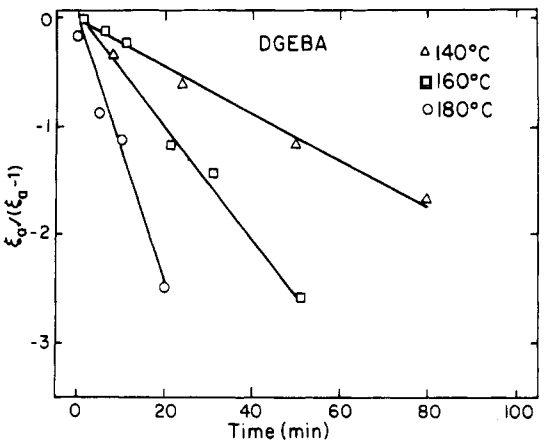

Figure 7. Plot of $\xi_a/(\xi_a - 1)$ vs. cure time to calculate rate constant (k_1) for epoxy–primary amine reaction.

One may ask what might have led to the small r values reported in a couple of cases[14,15] where IR spectroscopy or titration in a swollen network were used as the experimental techniques. In IR spectroscopy, it is extremely difficult to resolve primary amine from secondary amine. For the determination of the extent of cure, most researchers working on the characterization use the epoxy ring disappearance as a reasonably reliable method but not the amine peaks.[3,4] We will also describe the extent of cure on the basis of epoxy disappearance by IR in the last section. Titration in a swollen network can also suffer from experimental problems such as incomplete titration and degradation during the grinding process.

Now that the best-fit r value has been estimated, we will try to calculate k_1 from the kinetic equation (eq 2). In order to integrate eq 2, we need to express [b] (concentration of unreacted epoxy) and $[A_{pp}]$ in terms of ξ_a.[17]

By definition

$$1 - \xi_b \equiv [b]/4$$

Rearranging the above equation gives

$$[b] = 4 - 4\xi_b \tag{14}$$

In a stoichiometric mixture, $\xi_a = \xi_b$. For the case of $r = 1$, eq 13 is reduced to

$$\xi_a = 1 - [A_{pp}]^{1/4} \tag{15}$$

Rearranging eq 15 leads to

$$[A_{pp}] = (1 - \xi_a)^4 \tag{16}$$

Substituting eq 14 and 16 into eq 2, we get

$$-d(1 - \xi_a)^4/dt = 16k_1(1 - \xi_a)^5 \tag{17}$$

Rearrangement of eq 17 leads to

$$d\xi_a/(1 - \xi_a)^2 = 4k_1\, dt \tag{18}$$

Then we integrate to get

$$\xi_a/(\xi_a - 1) = -4k_1t \tag{19}$$

Figure 7 shows the plot of $\xi_a/(\xi_a - 1)$ vs. time for DGEBA–DDS epoxy at three cure temperatures. At cure times beyond gelation, the reaction rate constant, which is proportional to the slope of these curves, is clearly reduced. A similar decrease in the reaction rate has been observed by thermal analyses[17] and IR.[18] By drawing a straight line through the first few data points for the slope, we estimate k_1 to be 5.4×10^{-3}, 1.3×10^{-2}, and 3.1×10^{-2} min^{-1} at 140, 160, and 180 °C, respectively.

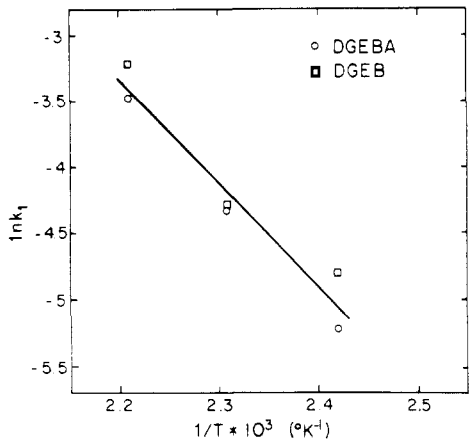

Figure 8. Arrhenius plot of ln k_1 vs. $1/T$.

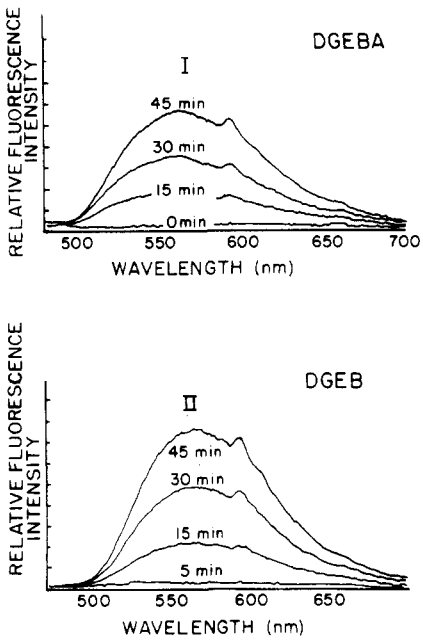

Figure 9. Fluorescence spectra of *p,p'*-diaminoazobenzene in a stoichiometric mixture of DGEBA–DDS (I) and DGEB–DDS (II) as a function of cure time at 160 °C (excitation at 456 nm).

Figure 8 shows an Arrhenius plot combining the data for both epoxy matrices. From the Arrhenius plot, an activation energy of 15.7 kcal/mol and a preexponential factor of 1.2×10^6 min^{-1} were estimated. These estimates from our studies are similar to reported values obtained by DSC and other techniques that measure the overall extent of reaction.[18,20-22]

4. Fluorescence Studies. When excited around 320 nm, both epoxy matrices are highly fluorescent with an emission maximum around 370–380 nm. When the fluorescence intensity is calibrated for thickness fluctuations, the fluorescence intensity is constant with the extent of cure. Therefore, the inherent fluorescence of the epoxy matrix itself is not useful to monitor cure reactions.

When the DAA label is excited, for example, at 456 nm, we observed a strongly cure dependent behavior of fluorescence intensity. Figure 9 shows such fluorescence spectra for DGEBA–DDS–DAA and DGEB–DDS–DAA epoxy matrices in the spectral range 450–800 nm. In both epoxy matrices, at zero cure time, hardly any fluorescence is observed. But with increasing cure time, fluorescence with a broad emission peak around 560 nm increases. At long cure times, the emission peak seems to have red-shifted slightly (by 5–10 nm). This small red shift is in sharp contrast to much larger red shifts observed in UV–vis

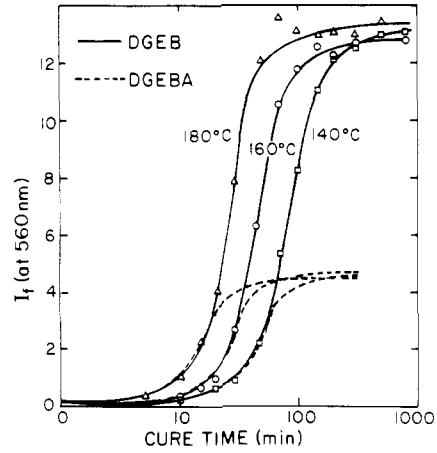

Figure 10. Relative fluorescence intensity at 565 nm as a function of cure time at three cure temperatures for DGEBA–DDS and DGEB–DDS epoxies.

spectra (refer to Figure 2I,II). Changes of polarity in the solvent medium are known to cause large shifts in emission spectra.[23,24] Therefore, we can conclude that polarity did not change much as the epoxy cured. This trend was also suggested by small shifts in UV–vis spectra by the model compound representing a cross-linker.

In order to quantify the fluorescence intensity changes, we plot relative fluorescence intensity at 560 nm (after dividing by the UV–vis peak area) as a function of cure time at three cure temperatures for both epoxies in Figure 10. Fluorescence intensity for DGEB epoxy is about the same as for DGEBA epoxy up to gelation time. However, fluorescence increases continuously beyond gelation for DGEB but levels off in DGEBA epoxy. This is due to vitrification, which occurs in DGEBA epoxy, but not in DGEB epoxy. In DGEBA epoxy, we have shown[9] that the increase in fluorescence originates from the cure products alone rather than from the viscosity changes. Thus the total fluorescence intensity can be written as $I_F = c\sum F_i A_i$, where F_i is the fluorescence intensity ratio obtained for each cure product under the same experimental conditions, A_i is their concentration, and c is the experimental constant. The fluorescence intensity ratio for the cross-linker model compound is found to be independent of cure. Using the concentration values obtained by deconvolution of UV–vis spectra (e.g., Table III), we found that a predicted I_F agrees well with the experimental points. Much greater values of I_F for DGEB are thus a direct consequence of further cure reactions as also indicated by UV–vis results as well as by IR monitoring of epoxy ring disappearance, which will be discussed in detail in the last section of this paper.

It will be useful to try to estimate the extent of cure reaction from the fluorescence intensity values. For this we proceed as follows: As described before, the total fluorescence intensity is attributed by the fluorescence of each cure product

$$I_F = c(F_{pp}A_{pp} + F_{ps}A_{ps} + F_{ss}A_{ss} + F_{pt}A_{pt} + F_{st}A_{st} + F_{tt}A_{tt}) \quad (20)$$

From the model compound studies,[25] the following fluorescence intensity ratio was estimated:

$$F_{pp}:F_{ps}:F_{ss}:F_{pt}:F_{st}:F_{tt} = 1:9:18:700:1100:1400$$

Thus

$$I_F = c(A_{pp} + 9A_{ps} + 18A_{ss} + 700A_{pt} + 1100A_{st} + 1400A_{tt}) \quad (21)$$

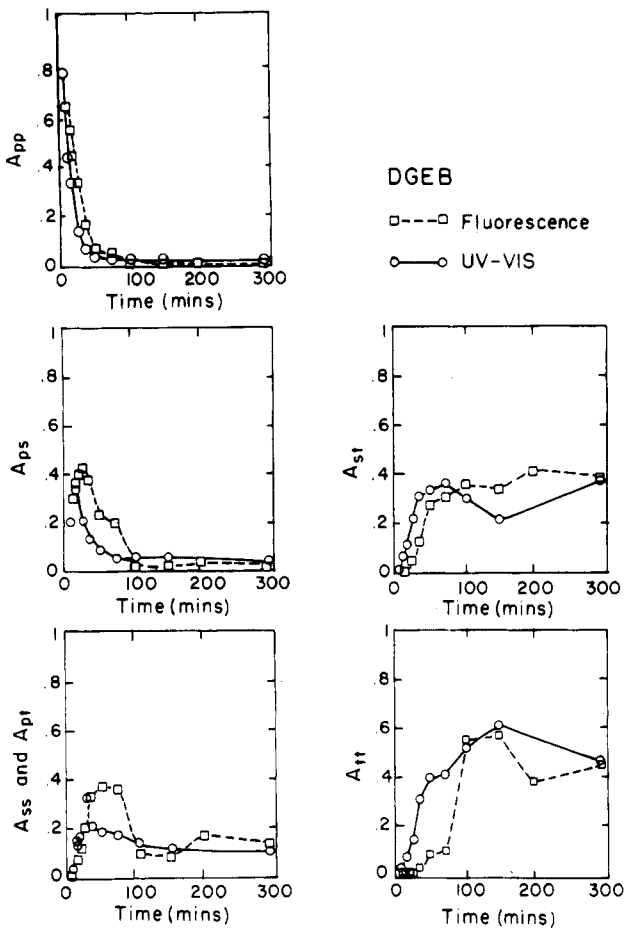

Figure 11. Comparison of cure compositions by UV–vis deconvolution and by fluorescence intensity.

Even though A_{pt} is usually smaller than A_{ss} when $r < 1$ (see Figure 5), we cannot ignore its contribution to fluorescence because F_{pt} is expected to be much larger than F_{ss}.

Substituting A_{ps}, A_{ss}, A_{pt}, A_{st}, and A_{tt} by A_{pp} and the amine reactivity ratio, r, according to eq 8–12, we obtain

$$I_F = c\{A_{pp} + 18p(A_{pp}^{q} - A_{pp}) + 18p^2(-2A_{pp}^{q} + A_{pp} + A_{pp}^{r/2}) + 700(-2pA_{pp}^{q} + rpA_{pp} + 2A_{pp}^{1/2}) + 1100p^2[(r+2)A_{pp}^{q} - rA_{pp} - (2-r)A_{pp}^{1/2} - 2A_{pp}^{r/2} + (2-r)A_{pp}^{r/4}] + 1400p^2[-rA_{pp}^{q} + (r^2/4)A_{pp} + (r/p)A_{pp}^{1/2} + A_{pp}^{r/2} - (2-r)A_{pp}^{r/4} + (r/2-1)^2]\} \quad (22)$$

Equation 22 shows that I_F is a function of only A_{pp} for a given r. Using $r = 1$, as determined from extensive data in the previous section, and the experimental constant c, estimated from a few sets of known compositions to be on the order of 0.01, we can determine A_{pp} for a given I_F using eq 22.

Once A_{pp} values are calculated, the concentration of other cure products can be calculated according to eq 8–12. Figure 11 shows a graphical representation of the data in comparison to the results obtained by UV–vis deconvolution. As can be seen, the cure composition obtained from fluorescence is in reasonable agreement with the data obtained by deconvolution of UV–vis spectra. Some discrepancies between the fluorescence and the UV–vis data are probably due to the error in the estimated fluorescence quantum yields of two cure species, A_{pt} and A_{st}.

In order to correlate fluorescence intensity at 565 nm with the overall extent of amine reaction, we plotted in Figure 12 I_F vs. ξ_a for both epoxies cured at three isothermal cure temperatures. In this figure, ξ_a is estimated from deconvolution of UV–vis spectra. All the data fall on a single smooth curve whose slope is much sharper at later stages of cure, especially after gelation. In other words, this fluorescence is a very sensitive monitoring technique for cure beyond gelation because its intensity comes mostly from tertiary amine products.

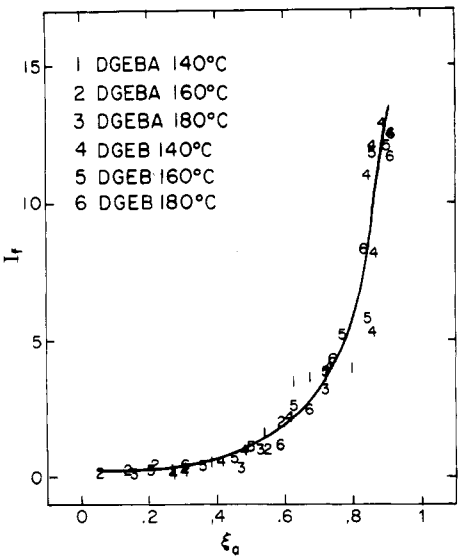

Figure 12. Correlation of relative fluorescence at 565 nm with the extent of amine reaction by UV–vis.

5. Molecular Weights and Soluble Fractions as a Function of Cure. By extending a recursive approach developed for ideal networks, Miller and Macosko derived molecular average properties of polymer networks in systems with first-shell substitution effects.[7] This applies in the epoxy–diamine system where the primary amine may have a different reactivity as compared with the secondary amine.

According to their theory, the weight-average molecular weight, $\bar{M}_w$, can be written for a stoichiometric mixture of epoxy–diamine as

$$\bar{M}_w = \{(1/2)[1 + \xi_a(4\xi_a - \mu + 1)]M_A^2 + [1 + \xi_a(\mu - 1)]M_B^2 + 4\xi_a M_A M_B\}/\{[(1/2)M_A + M_B][1 - \xi_a(\mu - 1)]\} \quad (23)$$

where ξ_a is the overall extent of cure reaction as defined by eq 1, M_A and M_B are the molecular weight of the diamine and the diepoxide, respectively, and μ is the weight-average extent of reaction as defined by

$$\mu = \frac{\sum i^2 A_i}{\sum i A_i} = \frac{A_{ps} + 4(A_{ss} + A_{pt}) + 9A_{st} + 16A_{tt}}{A_{ps} + 2(A_{ss} + A_{pt}) + 3A_{st} + 4A_{tt}} = \frac{A_{ps} + 4(A_{ss} + A_{pt}) + 9A_{st} + 16A_{tt}}{4\xi_a} \quad (24)$$

For our case, $M_A = 212$ (DAA) and $M_B = 202$ (DGEB) or 340 (DGEBA). According to eq 8–12, we can generate expected values of A_{ps}, A_{ss}, A_{pt}, A_{st}, and A_{tt} as a function of A_{pp} if r is known. For a given r value (we used 1 or 1.5), we have obtained a ξ_a (according to eq 1) and a corresponding μ value (according to eq 24) from each set of expected values of cure products.

These values (ξ_a and μ) are substituted in eq 23 to generate theoretical predictions of $\bar{M}_w$ as a function of ξ_a. Such predictions for DGEBA epoxy are shown as dotted lines in Figure 13 for two values of r. $\bar{M}_w$ does not change

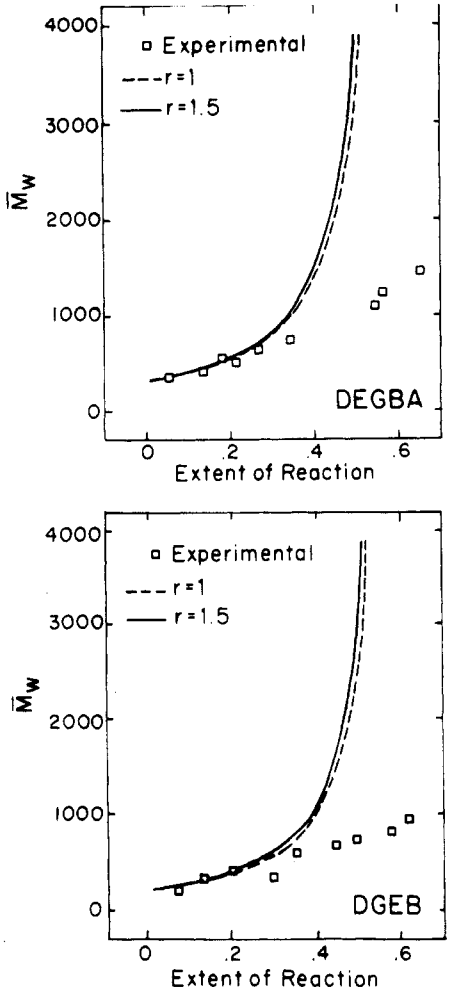

Figure 13. Comparison of predicted $\bar{M}_w$ with experimentally estimated values for DGEBA–DDS and for DGEB–DDS.

much whether it is 1 or 1.5 as shown by the closeness of the two solid lines.

Now we compare these theoretical predictions with our experimental data under a certain assumption. For our UV–vis curve deconvolution, we know the concentration of each of the cure products. In order to experimentally determine the molecular weight of the whole system, we need to know the molecular weight of each cure species. We assume that at early stages of cure (e.g., before gelation) only one side of diepoxide is reacted with diamine, leaving the other side unreacted in all cure products. This is a reasonable assumption when there are many unreacted diamines present, thus making molecular weight calculation of the cure species easy. With these molecular weight values of cure species (e.g., $A_{st} = M_A + 3M_B$) and compositional analyses (Table III), we can easily estimate $\bar{M}_w$ of the epoxy system as a function of ξ_a. The experimental values are indicated in the top panel of Figure 13 for DGEBA epoxy. Similar plots are shown in the bottom panel of Figure 13 for DGEB epoxy. In both panels experimental points follow closely the theoretical prediction in the early stages of cure. However, as the cure approaches gelation, experimental points are much smaller than predicted, since our assumption is not valid at higher conversion.

Now, we would like to see how predicted weight soluble fractions compare with some of the cure product compositions. Up to the gel point, all molecules are finite and therefore soluble. After the gel point, the weight soluble fraction, W_s, drops sharply. At 100% reaction, we expect

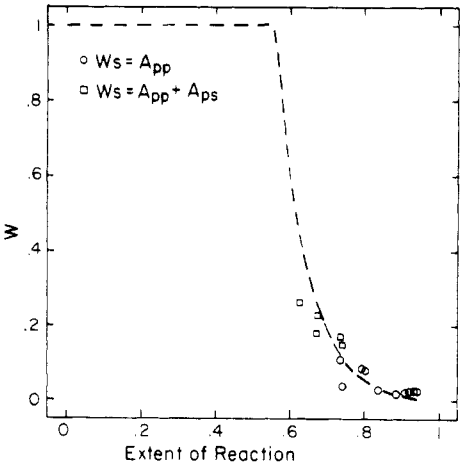

Figure 14. Comparison of predicted weight soluble fraction (smooth line) as a function of extent of amine reaction with composition of cure products.

to have an infinite network with no soluble species. Theoretical curves are first derived in Miller and Macosko's paper[26] and are extended by Charlesworth.[27] Part of the derivation as it applies to our system is

$$W_s = W_{Af}P(F_A^{out})^4 + W_BP(F_B^{out})^2 \quad (25)$$

where W_{Af} is the weight fraction of amine molecules, W_B is the weight fraction of epoxy molecules, $P(F_A^{out})$ is the probability that, looking out from an amine molecule, leads to a finite or dangling chain, $P(F_B^{out})$ is the probability that, looking out from an epoxy molecules, leads to a finite or dangling chain. $P(F_A^{out})$ and $P(F_B^{out})$ can be expressed in terms of the extent of reaction, ξ_a, for $f = 4$

$$P(F_A^{out}) = \left(\frac{1}{\xi_a} - \frac{3}{4}\right)^{1/2} - \frac{1}{2} \quad (26)$$

and then $P(F_B^{out})$ can be defined as

$$P(F_B^{out}) = \frac{P(F_A^{out}) - 1 + \xi_a}{\xi_a} \quad (27)$$

By substituting eq 26 and 27, we obtain

$$W_s = W_{Af}\left[\left(\frac{1}{\xi_a} - \frac{3}{4}\right)^{1/2} - \frac{1}{2}\right]^4 + \frac{W_B}{\xi_a^2}\left[\left(\frac{1}{\xi_a} - \frac{3}{4}\right)^{1/2} - \frac{3}{2} + \xi_a\right]^2 \quad (28)$$

The dotted line in Figure 14 shows the predicted weight soluble fraction, W_s, as a function of ξ_a according to eq 28. Also in Figure 14, some cure product compositions are indicated. At high cure conversion ($\xi_a > 0.8$, for example), W_s is only comparable to the unreacted DAA concentration (A_{pp}). This is quite reasonable since other cure products are expected to be incorporated into the network. At somewhat lower conversion ($\xi_a \sim 0.7$), the soluble fraction seems close to the added fractions of unreacted DAA (A_{pp}) and A_{ps}, which is the first product of the cure. This results illustrates the possibility of estimating the soluble fraction from cure product composition rather than from tedious and destructive solvent extraction studies.[27]

6. IR Studies and Comparison with UV–vis Studies. While our UV–vis and fluorescence studies follow the cure reactions from the amine functionality of DAA, IR spectroscopy can be used to monitor the cure from the epoxide functionality. Figure 15I plots the extent of epoxy

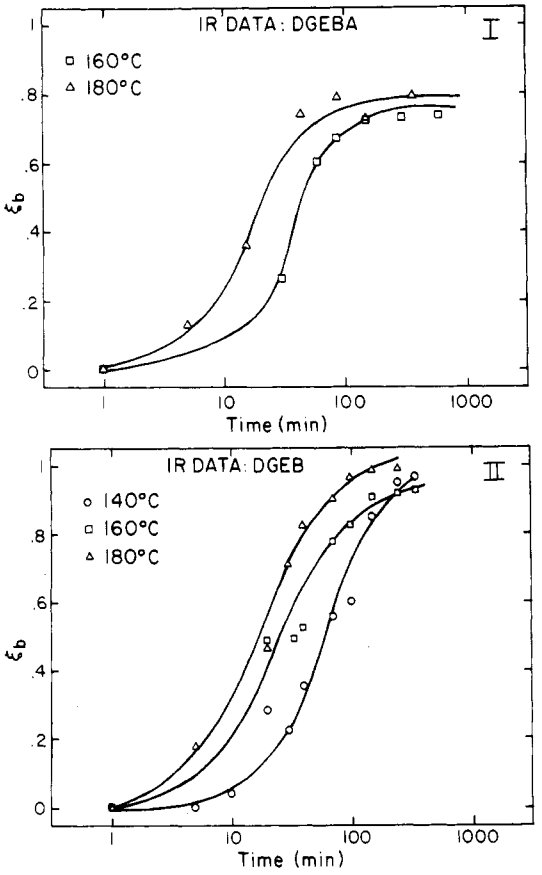

Figure 15. Extent of epoxy reaction as a function of cure time at 160 °C monitored by IR spectroscopy: (I) DGEBA–DDS; (II) DGEB–DDS.

reaction, ξ_b, for DGEBA–DDS epoxy as defined by the equation

$$\xi_b = 1 - \frac{A_{915cm^{-1}(t)}}{A_{1184cm^{-1}(t)}} \times \frac{A_{1184cm^{-1}(0)}}{A_{915cm^{-1}(0)}} \qquad (29)$$

where $A_{915cm^{-1}}$ is the IR absorption due to epoxy ring and $A_{1184cm^{-1}}$ is the absorption due to C–C stretching of the bridge carbon atom in DGEBA. For DGEB–DDS, $A_{1610cm^{-1}}$ due to the phenyl ring in DDS was used instead of $A_{1184cm^{-1}}$ as the internal standard to calibrate for thickness fluctuation during cure.[4] The curves in Figure 15I,II are also s-shaped, which shows strong cure temperature effects, especially in the early stages of cure. In DGEBA–DDS epoxy, the extent of epoxy cure, ξ_b, reaches about 80% maximum, while in DGEB–DDS epoxy, it reaches about 95% at 180 °C cure. In DGEBA–DDS epoxy, we also observe a leveling off at high conversion due to vitrification. When these epoxies are compared at the same temperature (e.g., 160 °C), greater cure is observed in DGEB–DDS than in DGEBA–DDS, which is consistent with UV–vis and fluorescence results.

In order to compare the extent of DAA amine reactions to epoxide reactions, we plotted ξ_a via UV–vis deconvolution vs. ξ_b for three cure temperatures. DGEB–DDS epoxy results are shown since we can monitor to almost complete reaction. The straight line in Figure 16 shows the slope of one which corresponds to the $\xi_a = \xi_b$ case. The data points in general indicate that ξ_a is somewhat greater than ξ_b, meaning faster consumption of DAA amine than of overall epoxide. Since most of the epoxide reacts with DDS, this type of behavior is an indication that DAA may react a little faster than DDS. In order to confirm such differences in the reactivity between DDS and DAA, we compare a scanning differential thermogram of a stoichiometric mixture of DGEB–DDS with that of DGEB–DAA, as shown in Figure 17. Even though the areas under the exotherm are not very different, DGEB–DAA epoxy has an exotherm at a lower temperature (about 20 °C lower), indicating a faster cure reaction by DAA than DDS. In other words, DAA gives a somewhat early warning signal ahead of DDS. Therefore, a calibration curve such as Figure 16 should be used in order to correlate the extent of reaction monitored by DAA with the extent of overall reaction in DDS containing epoxy.

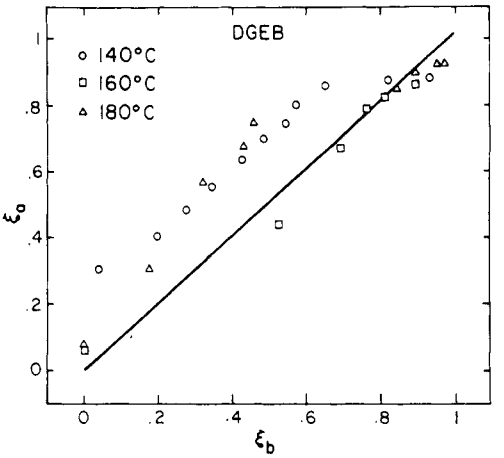

Figure 16. Plot of extent of amine reaction (ξ_a) vs. extent of epoxy reaction cured at three different temperatures for DGEB–DDS epoxy.

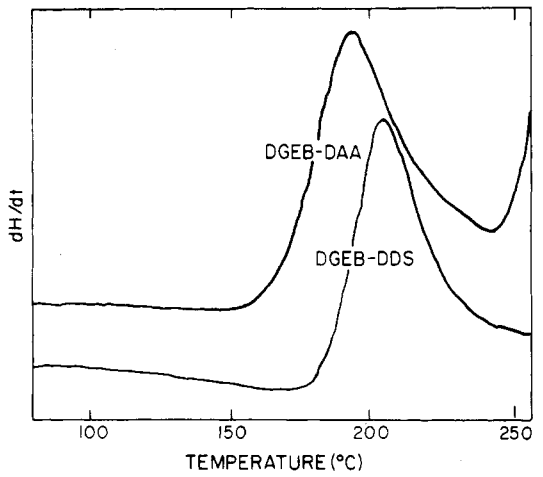

Figure 17. Thermogram of differential scanning colorimetry for a stoichiometric mixture of DGEB–DAA and DGEB–DAA at a heating rate of 10 °C/min.

Because of the upward curvature in Figure 16, relative insensitivity between ξ_a and ξ_b is expected, especially at high conversion. For example, when ξ_a is about 0.8, a 20% increase in ξ_a from 0.6 to 0.8 produces a change in ξ_a of only about 7% Such insensitivity is likely to be responsible for the unexpected similarity in the plateau values of ξ_a observed for DGEBA–DDS (Figure 4I) when it is cured at different temperatures.

Acknowledgment. We acknowledge the financial support of this work by the National Science Foundation, Polymers Program (Grant No. DMR82-05897), the Army Research Office (Contract No. DAA29-85-K-0055), and a grant from Hercules Co. Funding from the Institute of Materials and Science, University of Connecticut, and NSF toward the purchase of the new computerized instruments (diode array and fluorescence spectrometers) is also gratefully acknowledged. Several people have contributed to this work: C. Beretta and W. Yu in some fluorescence

measurements and P. Dickinson in some deconvolution analyses. Gratitude is extended to Professors J. Bobbitt and S. Huang for their help in model compound syntheses and for discussions in organic reactions and to Dr. G. Hagnauer, D. Dunn, and Dr. W. Zukas at AMMRC for their generous help in HPLC separation of model compounds and for stimulating discussions. We also acknowledge kind help from Professor H. Morawetz on the manuscript.

Registry No. DAA, 538-41-0; DDS, 80-08-0; DGEBA, 25085-99-8; DGEB, 29611-97-0; GPE, 122-60-1; 4-$H_2NC_6H_4N$=N-4-$C_6H_4NHCH_2CH(OH)CH_2OC_6H_5$, 105091-04-1; $C_6H_5OCH_2CH(OH)CH_2NH$-4-C_6H_4N=N-4-$C_6H_4NHCH_2CH(OH)CH_2OC_6H_5$, 105091-05-2; $(C_6H_5OCH_2CH(OH)CH_2)_2N$-4-$C_6H_4N$=N-4-$C_6H_4NH_2$, 105091-06-3; $(C_6H_5OCH_2CH(OH)CH_2)_2N$-4-$C_6H_4N$=N-4-$C_6H_4NHCH_2CH(OH)CH_2OC_6H_5$, 105091-07-4; $(C_6H_5OCH_2CH(OH)CH_2)_2N$-4-$C_6H_4N$=N-4-$C_6H_4N(CH_2CH(OH)CH_2OC_6H_5)_2$, 105091-08-5.

References and Notes

(1) Chin, I.-J.; Sung, C. S. P. *Macromolecules* **1984**, *17*, 2603.
(2) (a) Gordon, A. J.; Ford, R. A. *The Chemist's Companion*; Wiley: New York, 1972; pp. 146–147. (b) Exner, O. In *Correlation Analysis in Chemistry*; Chapman, N. B., Shorter, J., Eds.; Plenum: New York, 1978; Chapter 10, pp 469, 475.
(3) Enns, J. B.; Gillham, J. K. *Polymer Characterization*; Craver, C. D., Ed.; Advances in Chemistry Series 203; American Chemical Society: Washington, DC, 1983.
(4) Chang, T. D.; Carr, S. H.; Brittain, J. O. *Polym. Eng. Sci.* **1982**, *22*, 1213.
(5) (a) Dusek, K.; Ilavsky, M.; Lunak, S. *J. Polym. Sci., Polym. Symp.* **1975**, *No. 53*, 29. (b) Lunak, S.; Dusek, K. *J. Polym. Sci., Polym. Symp.* **1975**, *No. 53*, 45.
(6) Bidstrup, S. A.; Macosko, C. W. *Proceedings of ANTEC '84, SPE* **1984**, 278.
(7) Miller, D. R.; Macosko, C. W. *Macromolecules* **1980**, *13*, 1063.
(8) The deconvolution program is based on Gaussian probability functions as described in: *Data Reduction and Error Analysis in the Physical Sciences*; Bevington, P. R., Ed.; McGraw-Hill: New York, 1969.
(9) Sung, C. S. P.; Chin, I. J.; Yu, W.-C. *Macromolecules* **1985**, *18*, 1510.
(10) Prime, R. B. *Thermal. Characterization of Polymeric Materials*; Ed. Turi, E. A., Ed.; Academic: 1981; Figure 29, p 479.
(11) Byrne, C. A.; Hagnauer, G. L.; Schneider, N. S. *Polym. Comps.* **1983**, *4*, 206.
(12) See references cited in Table 1 of: Charlesworth, J. *J. Polym. Sci., Polym. Chem. Ed.* **1980**, *18*, 621.
(13) Zukas, W. X.; Schneider, N. S.; MacKnight, W. J. *Polym. Mater. Sci. Eng.* **1983**, *49*(2), 588.
(14) Bell, J. P. *J. Polym. Sci., Polym. Phys. Ed.* **1970**, *8*, 417.
(15) Morgan, R. J.; Happe, J. A.; Mones, E. T. *Proc. 28th SAMPE Symp.* **1983**, 596.
(16) Reference 10, p 443.
(17) We can calculate k_1 by expressing [b] in terms of [pp], followed by integration. However, it does not give as reliable values as those based on $[\xi_a]$.
(18) Riccardi, C. C.; Adabbo, H. E.; Williams, R. J. *J. Appl. Polym. Sci.* **1984**, *29*, 2481.
(19) Gupta, A.; Cizmecioglu, M.; Coulter, D.; Liang, R. H.; Yavrouian, A.; Tsay, F. D.; Moacanin, J. *J. Appl. Polym. Sci.* **1983**, *28*, 1011.
(20) Sourour, S.; Kamal, M. R. *Thermochim. Acta* **1976**, *14*, 41.
(21) Horie, K.; Hiura, H.; Souvada, M.; Mita, I.; Kambe, H. *J. Polym. Sci., Polym. Chem. Ed.* **1970**, *8*, 1357.
(22) Hagnauer, G. L.; Laliberte, B. R.; Dunn, D. A. *ACS Symp. Ser.* **1983**, *No. 221*, 231.
(23) Lippert, V. E. *Z. Elektrochem.* **1957**, *61*, 962.
(24) For a review see: Lakowicz, J. R. *Principles of Fluorescence Spectroscopy*; Plenum: New York, 1983; Chapter 7.
(25) The ratios for A_{pt} and A_{st} are estimated from the trends of observed ratios on A_{pp}, A_{pt}, A_{ss}, and A_{tt}. The ratio for A_{ss} was determined from fraction B.
(26) Miller, D. R.; Macosko, C. W. *Macromolecules* **1976**, *9*, 206.
(27) Charlesworth, J. M. *J. Polym. Sci., Polym. Phys. Ed.* **1979**, *17*, 1557.

Polymer Effects in Proton-Transfer Reactions. Poly(2-vinylquinoline)

M. R. Gômez-Antôn,[†] J. G. Rodríguez,[‡] and I. F. Piérola*[§]

Departamento Química General y Macromoléculas, Facultad de Ciencias, UNED, Ciudad Universitaria, 28040 Madrid, Spain, Departamento de Química Orgánica, Universidad Autonoma, 28049 Madrid, Spain, and Departamento Química Física, Facultad Ciencias Químicas, Universidad Complutense, 28040 Madrid, Spain. *Received April 28, 1986*

ABSTRACT: Emission, excitation, and absorption spectra of poly(2-vinylquinoline) and 2-methylquinoline solutions in dioxane–water mixtures have been measured as a function of the ionization degree, determined potentiometrically or spectrophotometrically. Absorption and excitation spectra give information about the ground-state equilibrium of heterocycle protonation. In the monomer analogue, the intensity of the emission coming from the protonated rings is proportional to the ground-state degree of ionization. Nevertheless, the emission coming from the heterocyclic protonated form in the polymer chain begins before the concentration of such a form would be measurable in the ground state. This is interpreted as being due to protonation of the ring following excitation as a consequence of the larger basicity of the heterocycle in the first singlet excited state when anchored in a polymer chain. The different behavior of the polymer and the monomeric model compound is interpreted in terms of the different approach to quinoline groups by solvent molecules.

Introduction

Chromophores that can undergo protonation usually have a dual emission[1,2] that is ascribed to the neutral and protonated forms. Ground-state protonation equilibrium is reflected in absorption and excitation spectra, although emission spectra are a consequence of excited-state behavior.

Ground state and excited state differ in their electronic configurations and as a consequence in their properties;[3] in particular, large basicity differences have been observed in heterocyclic systems of small molecules[2] but in only one polymer case.[4] When an aromatic heterocycle is excited, the ground-state equilibrium of protonation is perturbed

[†] UNED.
[‡] Universidad Autonoma.
[§] Universidad Complutense.

0024-9297/86/2219-2932$01.50/0